Fischer, Andreas ; Stöbener, Dirk

In-process roughness quality inspection for metal sheet rolling

Journal Article	as:	peer-reviewed accepted version (Postprint)
DOI of this document*(secondary publication):		https://doi.org/10.26092/elib/3318
Publication date of this document:		13/09/2024

* for better findability or for reliable citation

Recommended Citation (primary publication/Version of Record) incl. DOI:

Andreas Fischer, Dirk Stöbener, In-process roughness quality inspection for metal sheet rolling, CIRP Annals, Volume 68, Issue 1, 2019, Pages 523-526, ISSN 0007-8506, https://doi.org/10.1016/j.cirp.2019.04.069.

In-process roughness quality inspection for metal sheet rolling

Andreas Fischer *, Dirk Stöbener

Bremen Institute for Metrology, Automation and Quality Science (BIMAQ), MAPEX Centre for Materials and Processes, University of Bremen, Bremen, Germany

Submitted by Bernd Scholz-Reiter (1)

Keywords:
Metrology
Roughness
Optical

1. Introduction

The quality of fine-rolled sheets depends to a significant extent on the surface quality of the work rolls, which are subject to continuous wear. Therefore, regular reconditioning of these rolls is necessary in order to ensure a constant surface quality of the sheets. The occurring wear differs locally over the roll surface and its dimension normal to the surface is in the low micrometer or nanometer range. Hence, every section of the roll surface must be inspected and, if necessary, machined during the reconditioning process. The surface assessment of the rolls during reconditioning is currently performed as a non-automated, visual inspection by the operator. Therefore, as a first step towards an automatic control of the reconditioning process, an in situ capable surface quality sensor has to be developed for inspecting large surface areas in a short time in the order of $>0.5\,m^2/min$.

Commonly applied tactile probes cannot meet the speed requirement and can lead to damages on the smooth roll surfaces. Furthermore, common optical topography measurements such as with white light interferometry are too slow due to the necessary scanning over the large roll dimensions of typically $0.3-0.6\,m \times 0.7-1.2\,m$. However, optical scattered light measurement techniques can meet the measurement demands [1], and especially speckle-based methods are known to measure and evaluate the surface roughness of large areas at high speed [2,3].

1.1. Optical roughness measurement techniques

The measuring effect of the speckle roughness measurement techniques is based on the determination of the statistical properties of the speckle patterns generated by the illuminated rough surface. Goodman showed theoretically that the roughness of a coherently illuminated and observed surface influences the contrast of the resulting speckle images and suggested contrast-based measurement systems [4]. As the surface roughness of the rolls is less than 1/8 of the illumination wavelength, partially developed speckle patterns with lowered contrast ratios occur [5], which prevent a successful application of these systems on the working rolls. Yoshimura et al. and Lehmann presented theoretical approaches for speckle-based measurement principles using an already speckled illumination of the investigated surface [6,7]. Yoshimura et al. investigated the application of the measurement principle at transmitting isotropic surfaces [8] whereas Lehmann also considered reflecting and anisotropic surfaces [7]. Both approaches use the autocorrelation function of the observed speckle images to evaluate their roughness depending intensity modulations.

Despite the principle demonstration of speckle-based roughness measurement sensors in laboratory experiments, only a few applications for measurements on manufactured surfaces were reported until today. Pino et al. presented an approach for the determination of the roughness of manufactured paper sheets [9] and Dhanasekar et al. showed investigations regarding the measurement of ground and milled surfaces [10]. However, the application and characterization of speckle-based measurement systems for optical roughness measurements of smooth and curved metal surfaces with a large measurement zone and a high measurement speed needed to establish an automated reconditioning process for working rolls is still an open task.

1.2. Aim and outline

The aim of this article is the experimental proof that an optical, speckle-based roughness sensor meets the requirements in terms of speed and measurement uncertainty for the in situ investigation of working rolls for fine rolling processes during reconditioning. Note that the paper particularly focusses on the evaluation and

* Corresponding author.
E-mail address: andreas.fischer@bimaq.de (A. Fischer).

interpretation of the measurement results. Section 2 describes shortly the sensor measurement principle, the data evaluation, the calibration to standardized roughness values as well as the results of a theoretical uncertainty estimation. The operating environment, the process and measurement requirements as well as the realized sensor setup are explained in Section3. The measurement results including an experimental uncertainty evaluation are subsequently discussed in Section 4 and the conclusions and an outlook are presented in Section 5.

2. Speckle-based roughness measurement

2.1. Measurement principle

The measurement principle of the fast, speckle-based roughness sensor system is depicted in Fig. 1. A collimated and pulsed laser beam with a Gaussian intensity profile illuminates the sample surface under a small inclination angle. The reflected light is captured with a lensless camera in the far field (Fraunhofer region) and the captured, partially developed speckle pattern with roughness depending intensity modulations are evaluated by image processing algorithms regarding the average roughness of the illuminated measuring spot.

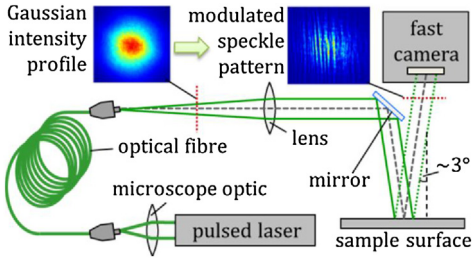

Fig. 1. Schematic illustration of the measurement principle.

2.2. Image processing

The surface roughness expressed as the optical roughness value *Ropt* is characterized by fast image processing of the recorded speckle image intensity modulations. The *Ropt* value is determined in three calculation steps as shown in Fig. 2 [2].

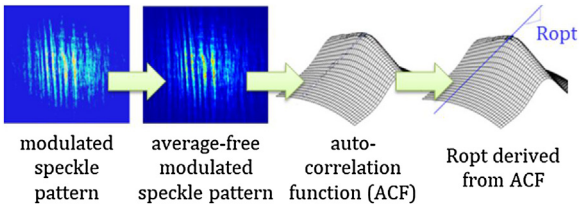

Fig. 2. Evaluation scheme of the roughness sensor.

First, the algorithm subtracts the mean intensity offset from the speckle image and then determines the autocorrelation function (ACF) γ of the average-free image:

$$\gamma(\Delta m,\ \Delta n) = \frac{\sum_{m=1}^{M}\sum_{n=1}^{N}[(I(m,n)-\bar{I})\cdot(I(m+\Delta m,\ n+\Delta n)-\bar{I})]}{\sum_{m=1}^{M}\sum_{n=1}^{N}[I(m,n)-\bar{I}]^2}.$$

I(m, n) represents the pixel intensity at the pixel position (m, n), M and N describe the number of pixels in x- and y-direction of the image, $\bar{I}$ is the average intensity of each image and Δm, Δn give the displacement for the calculation of the ACF in unit pixel.

Subsequently, the *Ropt* value is calculated. Its value is the slope of the ACF in the immediate vicinity of the ACF centre. The calculation is performed in the lateral surface direction desired for the roughness measurement, which is described by the vector ($\Delta\tilde{m}$, $\Delta\tilde{n}$) in the ACF's coordinate system

$$Ropt(\Delta\tilde{m},\Delta\tilde{n}) = \frac{1-\gamma(\Delta\tilde{m},\ \Delta\tilde{n})}{\sqrt{\Delta\tilde{m}^2+\Delta\tilde{n}^2}}.$$

The root $\sqrt{\Delta\tilde{m}^2+\Delta\tilde{n}^2}$ describes the chosen evaluation distance from the ACF centre in unit pixels for determining the slope. Since the shape of the ACF varies in the vicinity of its centre (cf. Fig. 2), the evaluation distance affects the resulting *Ropt* value [3]. Therefore, $\Delta\tilde{m}$ and $\Delta\tilde{n}$ are selected so that the sensitivity of the roughness measurement system is maximized for the intended measuring range.

2.3. Roughness calibration

The *Ropt* values (as empirically calculated values) do not linearly correlate with the standardized roughness values such as *Sa* or *Sq*. Hence, a sensor calibration with respect to a standardized roughness value is necessary. This calibration is valid only for the used ACF evaluation parameters $\Delta\tilde{m}$ and $\Delta\tilde{n}$, because of their mentioned influence on the Ropt values (cf. Section 2.2). The calibration also depends on the used filtering parameters for the calculation of standardized roughness values from micro-topography measurements according to ISO 25178 [11]. Note that no theoretical relationship between the ACF evaluation parameters and the filtering parameters exists. In the presented application on the work rolls, a calibration to standard *Sa* values with the ACF evaluation parameters $\Delta\tilde{m}=2$ and $\Delta\tilde{n}=0$ was chosen. For this purpose, 100 repeated measurements were carried out on five reference samples with different surface roughness, which correspond to the surface structure of the rolls and represent the expected roughness range. The mean values $Ropt_{cal}$ for each sample were compared with reference Sa_{cal}-values determined from topography measurements with a chromatic confocal distance sensor in the same measuring regions on the reference samples. Fig. 3 shows the results of the sensor calibration in the range from $Sa_{cal}=3$ nm to $Sa_{cal}=78$ nm.

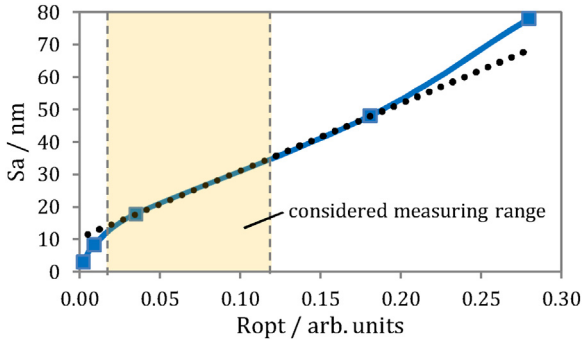

Fig. 3. Calibration of the measurement system determined by comparison with reference data. The dotted line represents the linear calibration for the considered measuring range. Note that the uncertainties of the data points are smaller than the plotted square markers.

A clear non-linear behaviour of the calibration curve occurs in particular in the *Sa* range below 15 nm. When applied to the work rolls, however, *Sa* values in the range between 15 and 35 nm are expected. Therefore, the sensor must only be calibrated for this range, which can be approximated by the linear relation

$$Sa = f(Ropt) = a\cdot Ropt + b$$

with the slope $a=(206.509\pm0.192)$ nm/a.u. and the axial intercept $b=(10.613\pm0.025)$ nm, see dotted line in Fig. 3. The uncertainties of the slope and the intercept are derived according to [12] from the standard deviation $s(Ropt_{cal})=0.0002$ a.u. of the $Ropt_{cal}$ calibration measurements and the uncertainty $u(Sa_{cal})=0.2$ nm of the reference roughness measurements given by the reference sensor manufacturer.

2.4. Theoretical measurement uncertainty

The uncertainty of the measured roughness values is calculated via uncertainty propagation according to [12] with

$$u(Sa) = \sqrt{\underbrace{\sum_{m=1}^{M}\sum_{n=1}^{N}\left(\frac{\partial Sa}{\partial Ropt}\cdot\frac{\partial Ropt}{\partial \gamma}\cdot\frac{\partial \gamma}{\partial I(m,n)}\cdot u\left(I(m,n)\right)\right)^2}_{=u_I^2(Sa)} + \ldots + \underbrace{\left(\frac{\partial Sa}{\partial a}\cdot u(a)\right)^2 + \left(\frac{\partial Sa}{\partial b}\cdot \mathrm{u(b)}\right)^2}_{=u_{cal}^2(Sa)}}$$

including the uncertainty contributions $u_I(Sa)$ from the measured speckle images and $u_{cal}(Sa)$ resulting from the sensor calibration ($u(a)$ and $u(b)$, see Section 2.3).

In order to obtain an estimation for the theoretically achievable, minimum measurement uncertainty $u_{min}(Sa)$ of the system, it is assumed that the components of the sensor system work ideally and that all systematic deviations are covered by the calibration. Hence, only random, physically unavoidable sources of uncertainty have to be considered for the calculation of $u_{I,min}(Sa)$. The following random influences on the measured pixel intensities I, which contribute via the evaluation of the speckle images to $u_{I,min}(Sa)$, were taken into account: photon noise of the laser, readout noise of the camera pixels, dark current noise and intensity quantization during the A/D conversion of the recorded intensities. The examination showed that the photon shot noise and the signal quantization make by far the largest random contributions to the minimum measurement uncertainty of the considered sensor system. The dominant source is photon shot noise, while quantization gains a significant influence only for low mean intensities. The contribution of dark current and readout noise is negligible [3]. The total contribution of the considered random influences amounts to $u_{I,min}(Sa) = 0.04$ nm.

This value is raised by the influences of the calibration parameter uncertainties $u(a)$ and $u(b)$. Their summed contribution $u_{cal,min}(Sa)$ is almost as large as the contribution $u_{I,min}(Sa)$, so that the influence of the calibration on the uncertainty cannot be neglected. For the setup used in these investigations, an estimated total uncertainty of $u_{min}(Sa) < 0.06$ nm results for the relevant roughness value range of 15 nm–35 nm.

3. Experimental measurement setup

The in situ measurement capability of the speckle-based roughness sensor is tested with three different measurement series on one roll in a reconditioning station for fine-rolling working rolls. The first measurement series was captured at one surface position of the non-rotating working roll in order to estimate the sensor's uncertainty in the application environment for repeated measurements. The other two measurement series were carried out to investigate the comparability of measurements on rotating rolls and to find out whether the rotational speed has an influence on the measurement results.

3.1. Process environment and requirements

The reconditioning station is located on the shop floor level and is able to treat rolls with diameters of 60 cm and length of up to 1.2 m. The aim of the reconditioning treatment is to restore a cylindrical geometry of the roll with a homogeneous surface roughness below 30 nm. Therefore, the sensor should exhibit a measurement uncertainty of the roughness value Sa below 0.5 nm and should reach a measuring speed of 0.5 m^2/min to avoid long measuring times. The station is equipped with a linear guide to move the tool in axial direction along the working roll. During the measurements, the tool is replaced by the sensor.

3.2. Measurement setup

The measurement setup consists of a pulsed laser light source (wavelength $\lambda = 532$ nm, pulse length < 10 µs), which is coupled to a 5 m single-mode fibre in order to generate the homogeneous Gaussian beam profile. The beam is collimated and widened to a measurement spot diameter of 10 mm by a lens system and directed to the measured surface by a mirror. The specular reflected light is captured by a camera (Sentech STC-CMB2MCL, 8 bit resolution) without a lens as illustrated in Fig. 1. The mirror is adjusted to a measuring distance of 100 mm and the camera is connected via a fast cameralink interface to a FPGA-based image evaluation board, which processes the images pipe-wise pixel by pixel. This configuration ensures evaluation frequencies of up to 340 Hz. In order to avoid motion blur, the triggering of the pulsed laser and the camera is adjusted in such a way that pixel illumination times of less than 1 µs result.

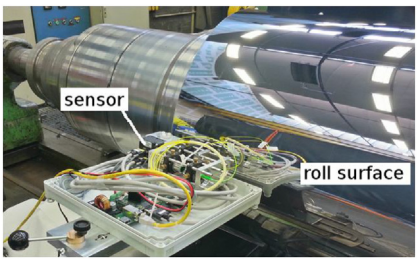

Fig. 4. Working roll in reconditioning station with roughness sensor.

The data acquisition was not triggered with the rotational position of the working roll, so that it could not be ensured that an integer average number of measurement points was recorded per roll revolution. Fig. 4 shows the sensor setup mounted on the linear guide next to the specular reflecting surface of the working roll in the reconditioning station.

4. Results and discussion

4.1. Measurements on stationary roll

The measurement series with 3300 measurements performed on a stationary roll shows an empirical standard deviation of about 0.22 nm, which is clearly above the theoretically estimated, minimum measurement uncertainty $u_{min}(Sa)$. An investigation of the recorded speckle images revealed, that the larger uncertainty results from intensity profile fluctuations of the used laser, which influence the mean intensity value. Since no such fluctuations were observed during the calibration measurements in the laboratory, it is assumed that the fluctuations are triggered by variations of the conditions in the production environment.

Due to the pipe structure of the data processing in the FPGA, the required direct subtraction of the intensity mean value is not possible, so that the subtracted value is estimated from the values of the previous images. As a result, the intensity fluctuations influence the autocorrelation functions and thus the measured roughness value. This influence could only be eliminated by changing the evaluation algorithm, which would reduce the measurement frequency (and thus the measurement speed) to a not acceptable level for the reconditioning process.

Despite the additional influences, the measurement uncertainty of the sensor system for a stationary roll $u_{stat}(Sa) = 0.22$ nm is still below the 0.5 nm limit required for the application.

4.2. Measurements at $v = 15.5$ m/min

In the first series with a rotating roll, about 10,000 measurement points were acquired with 200 Hz during 6.5 revolutions of the roll. The aim was to assess the repeatability of the measurements between the revolutions of the roll. The rotating roll's low surface speed of $v = 15.5$ m/min leads to an overlap in circumferential direction of 8.7 mm between two successive measurement zones with a diameter of 10 mm. This was chosen to prevent strong changes in the roughness signal, aggravating the comparability estimation. Fig. 5 shows the roughness measurement results plotted against the rotational position of the roll for the 6 successive revolutions.

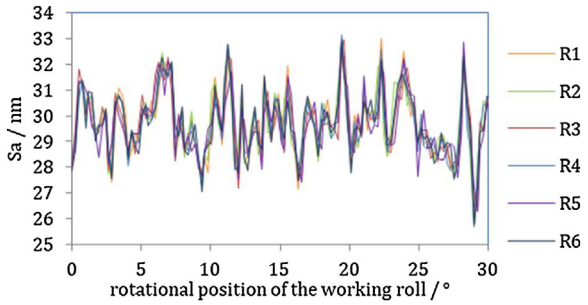

Fig. 5. Measured roughness values for the rotational position range of 0°–30° of the working roll for a rotational frequency of 8.22 rpm (v = 15.5 m/min) measured on consecutive revolutions (R1–R6).

The section between 0° and 30° is shown in Fig. 5 as an example and in order to ease the visual estimation of the comparability. The measured roughness deviations between corresponding rotational positions are much smaller than the observed variations of the measured roughness values in circumferential direction during one roll revolution. Hence, the observable roughness behaviour in circumferential direction is not caused by measurement uncertainties, but reflects the local variation of the surface roughness of the roll.

In order to assess the sensor characteristic for the moving roll surface, the changes of the measured data from revolution to revolution were evaluated. The empirical standard deviation of these changes amounts to $u_{slow}(Sa) = 0.41$ nm, which is above the variation for the stationary roll. The uncertainty increase can be explained by the missing sensor trigger (cf. Section 3.2). The lack of triggering to fixed rotation positions of the roll leads to displacements of the measurement zone positions of up to 4 mm in circumferential direction on the roll surface. In combination with the existing roughness variations of the roll surface, these measuring zone shifts lead to additional variations of the measured roughness values. Despite the increased roughness standard deviation, the required measurement uncertainty of $<$0.5 nm is achieved also on moving roll surfaces.

4.3. Measurements at v = 87 m/min

In order to demonstrate a surface measurement speed of $>$0.5 m^2/min, a measurement with 200 Hz frequency on a fast rotating roll with a surface speed of v = 87 m/min (corresponding to 0.77 m^2/min) was performed. Fig. 6 shows a section of the measured roughness values of 8 consecutive revolutions plotted against the rotational position of the roll. In agreement to the measurements with v = 15.5 m/min, the variations in the circumferential direction are significantly larger than the differences between the values of the individual revolutions. Hence, the observed roughness variations mainly originate from the surface roughness variation on the working roll.

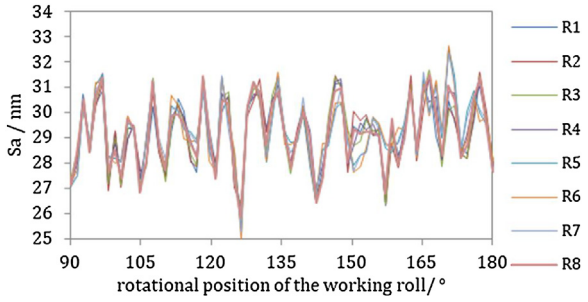

Fig. 6. Roughness values for the rotational position range of 90°–180° of the working roll for a rotational frequency of 46.15 rpm (v = 87.0 m/min) measured on consecutive revolutions (R1–R8).

However, the detected period of the roughness measurements is not one but three revolutions of the roll. Since this phenomenon only occurs at the high roll rotational speed and the rolls have a high mass due to their internal structure and diameter of 60 cm, it is assumed that a wobbling movement of the roll due to imbalances and bearing play occurs. The axial component of the wobble motion causes the surface measuring profile to return to its initial position after three roll revolutions. The superposition of the axial and the circumferential (cf. Section 4.2) measurement zone displacements in combination with the surface roughness variations of the roll leads to the observed roughness values with a periodicity over three roll revolutions. Finally, the standard deviation of the roughness values amounts to $u_{fast}(Sa) = 0.45$ nm, which is similar to the measurements at v = 15.5 m/s.

In summary, all measurements show variations, which are smaller than the specified uncertainty limit of 0.5 nm.

5. Conclusions

The presented system offers the possibility to perform fast roughness measurements with a measuring spot of 10 mm diameter on smooth surfaces with *Sa* roughness values below 80 nm. Its applicability for in situ measurements during the reconditioning of work rolls for finishing processes was demonstrated by measurements on a static roll and a roll rotating at different speeds. The measurements on the non-rotating roll showed a measurement uncertainty of 0.22 nm, which is only by a factor of 3 higher than the estimated minimum uncertainty. It was elaborated, that these differences mainly result from observed mean intensity variations between the captured speckle images. They influence the roughness evaluation algorithm, which could not be adapted to this problem without decreasing the measurement frequency, required by the application.

During the measurements on the rotating roll, the measuring system was able to reproduce the roughness variations during several revolutions with uncertainties lower than 0.5 nm. The uncertainty increase compared to the stationary roll could be mainly attributed to the lack of sensor triggering on the rotational position of the roll. In addition, no significant velocity influence on the roughness uncertainties could be observed. This very good comparability of the surface values, which was even achieved at a surface measurement speed of 0.77 m^2/min, confirms the applicability of the measuring principle for the in situ use on working rolls for rolling processes. Consequently, the sensor system can be used in the future to establish an automated and controlled surface treatment of the work rolls.

Acknowledgements

The project on which this article is based was funded by the Federal Ministry of Education and Research under the number 13N13535. The authors are responsible for the content of this publication. The authors thank C. Stehno and T. Eilts from CoSynth GmbH and L. Gerth from Hille & Müller GmbH as well as S. Patzelt (University of Bremen) for their support regarding the measurements of the working roll during reconditioning.

References

[1] Lehmann P, Goch G (2000) Comparison of Conventional Light Scattering and Speckle Techniques Concerning an in-process Characterization Of Engineered Surfaces. *Annals of the CIRP* 49(1):419–422.
[2] Patzelt S, Horn F, Goch G (2006) Fast Integral Optical Roughness Measurement of Specular Reflecting Surfaces in the Nanometer Range. *XVIII IMEKO World Congress — Metrology for a Sustainable Development*.
[3] Patzelt S, Stöbener D, Ströbel G, Fischer A (2017) Uncertainty of Scattered Light Roughness Measurements Based on Speckle Correlation Methods, SPIE Optical Metrology. *Proceedings of SPIE* 10329. No. 103291P.
[4] Goodman JW (1975) Dependence of Image Speckle Contrast on Surface Roughness. *Optics Communications* 14(3):324–327.
[5] Ogilvy A (1991) *Theory of Wave Scattering from Random Rough Surfaces*, Hilger.
[6] Yoshimura T, Kato K, Nakagawa K (1990) Surface-roughness Dependence of the Intensity Correlation Function Under Speckle Pattern Illumination. *Journal of the Optical Society of America* 7(12):2254–2259.
[7] Lehmann P (1999) Surface-roughness Measurement Based on the Intensity Correlation Function of Scattered Light Under Speckle-Pattern Illumination. *Applied Optics* 38(7):1144–1152.
[8] Yoshimura T, Miyazaki E, Naka K (1993) Monitoring Surface Roughness by Means of Doubly Scattered Image Speckle. *Optical Engineering* 32:1354–1359.
[9] Pino A, Pladellorens J, Cusola O, Caum J (2011) Roughness Measurement of Paper Using Speckle. *Optical Engineering* 50(9):093605.
[10] Dhanasekar B, Mohan NK, Bhaduri B, Ramamoorthy B (2008) Evaluation of Surface Roughness Based on Monochromatic Speckle Correlation Using Image Processing. *Precision Engineering* 32:196–206.
[11] ISO 25178-3 (2012) *Geometrical Product Specifications (GPS) – Surface Texture: Areal*, Beuth.
[12] JCGM100 (2008) Evaluation of Measurement Data—Guide to the Expression of Uncertainty in Measurement. *BIPM*.